Electronic structure and energetics of the tetragonal distortion for TiH_2, ZrH_2, and HfH_2: A first-principles study

Ramiro Quijano and Romeo de Coss
Departamento de Física Aplicada, Centro de Investigación y de Estudios Avanzados del IPN, Unidad Mérida A.P. 73 Cordemex, Mérida, Yucatán 97310, Mexico

David J. Singh
Materials Science and Technology Division, Oak Ridge National Laboratory, Oak Ridge, Tennessee 37831-6114, USA
(Received 16 December 2008; revised manuscript received 2 October 2009; published 10 November 2009)

The electronic structure and energetics of the tetragonal distortion for the fluorite-type dihydrides TiH_2, ZrH_2, and HfH_2 are studied by means of highly accurate first-principles total-energy calculations. For HfH_2, in addition to the calculations using the scalar relativistic (SR) approximation, calculations including the spin-orbit coupling have also been performed. The results show that TiH_2, ZrH_2, and HfH_2 in the cubic phase are unstable against tetragonal strain. For the three systems, the total energy shows two minima as a function of the c/a ratio with the lowest-energy minimum at $c/a<1$ in agreement with the experimental observations. The band structure of TiH_2, ZrH_2, and HfH_2 (SR) around the Fermi level shows two common features along the two major symmetry directions of the Brillouin zone, $\Gamma-L$ and $\Gamma-K$, a nearly flat doubly degenerate band, and a van Hove singularity, respectively. In cubic HfH_2 the spin-orbit coupling lifts the degeneracy of the partially filled bands in the $\Gamma-L$ path, while the van Hove singularity in the $\Gamma-K$ path remains unchanged. The density of states of the three systems in the cubic phase shows a sharp peak at the Fermi level. We found that the tetragonal distortion produces a strong reduction in the density of states at the Fermi level resulting mainly from the splitting of the doubly-degenerate bands in the $\Gamma-L$ direction and the shift of the van Hove singularity to above the Fermi level. The validity of the Jahn-Teller model in explaining the tetragonal distortion in this group of dihydrides is discussed.

DOI: 10.1103/PhysRevB.80.184103 PACS number(s): 64.70.K−, 71.15.Nc, 71.20.Be, 71.15.Rf

I. INTRODUCTION

Many transition metals react with hydrogen to form stable metal hydrides.[1] The typical structure of the transition-metal dihydrides (MH_2) is the CaF_2 crystal structure, where the metal atoms form a face-centered-cubic (fcc) sublattice and the hydrogen atoms occupy the tetrahedral lattice sites. Nevertheless, the ground state of the group IV dihydrides TiH_2, ZrH_2, and HfH_2 is a tetragonally distorted fluorite structure (space group No. 139), which is basically a face-centered-tetragonal (fct) cell structure with $c/a<1$.[1–8] For TiH_2, ZrH_2, and HfH_2, the measurement of the c/a ratio at low temperatures is 0.945, 0.890, and 0.898, respectively.[2,3,6,8] Interestingly, upon heating TiH_2 shows a tetragonal-cubic structural transition at a critical temperature of 310 K, with practically no change in volume.[3] Thus, the observed deviation from the ideal CaF_2 structure for the metal-dihydrides TiH_2, ZrH_2, and HfH_2 shows that the cubic phase is unstable at low temperatures.

From the theoretical point of view, the study of the energetics for the tetragonal distortion in the Ti and Zr dihydrides has been addressed only recently. Ackland[9] found an almost degenerate double minimum potential for ZrH_2, using a pseudopotential method, obtaining the ground state for $c/a>1$, in clear disagreement with the experimental data.[3–8] On the other hand, Wolf and Herzig[10] performed full-potential LAPW calculations using the local density approximation for TiH_2 and ZrH_2, in which they studied the total energy as a function of the c/a ratio. For TiH_2, they found that the ground state is at $c/a>1$, in contradiction with experimental observation,[3] while for ZrH_2 they obtained the correct ground state ($c/a<1$). More recently, similar studies were done by Xu and Van der Ven[11] for TiH_2 using the pseudopotential method, obtaining the correct ground state for this system ($c/a<1$). It is important to mention that previous calculations of the tetragonal distortion in TiH_2 and ZrH_2 show that the fct-fcc energy barrier is very small.[9–11] In particular, for TiH_2 the energy difference between the fcc and fct structures is only a fraction of 1 mRy.[10,11] Thus, highly accurate calculations are needed for studying the tetragonal distortion in this group of dihydrides. With respect to HfH_2, to our best knowledge, the energetics of the fcc-fct structural transition has not been previously reported.

The current explanation of the tetragonal distortion in TiH_2, ZrH_2, and HfH_2 is given in terms of an electronic-driven instability of the cubic phase resulting from a very high density of states at the Fermi level.[12–19] Self-consistent band structure calculations have showed that TiH_2, ZrH_2, and HfH_2 in the cubic phase have a high density of states at the Fermi level, $N(E_F)$, which has been associated to a doubly degenerate band in the $\Gamma-L$ direction.[10,20,22,23] Thus, the structural instability of the cubic phase in TiH_2, ZrH_2, and HfH_2 is interpreted as a Jahn-Teller effect driven by the splitting of the bands at the Fermi level.[10,17,23,24] Nevertheless, in that analysis the spin-orbit coupling effects on the band structure was neglected. The spin-orbit coupling is important for heavy elements such as Hf,[25,26] and it is expected that the spin-orbit coupling lifts the degeneracy of the partially filled bands in the particular case of fcc-HfH_2.[20,21] Hence, the validity of the Jahn-Teller model for the tetragonal distortion in

HfH_2 is questionable, since the doubly-degenerate band at the Fermi level is no longer present in the cubic phase. However, to our best knowledge, band-structure calculations for HfH_2 taking the spin-orbit coupling into account have not been reported previously. It is important to mention that in order to explain the tetragonal distortion in TiH_2 and ZrH_2, an electronic-driven mechanism different to the Jahn-Teller effect has been suggested in the literature.[22,27] In particular, Kulkova *et al.*[22] have showed that the weakly dispersive segments of the energy bands along $\Gamma-L$ does not play an exclusive role in the strong reduction in $N(E_F)$ during the cubic-tetragonal distortion of TiH_2 and ZrH_2, and they have concluded that the reduction in the DOS at $E-F$ must be supplemented by a shift in energy of the band along the $\Gamma-K$ direction. In view of the contrasting conclusions reported in the literature about the origin of the structural instability of titanium and zirconium dihydrides in the cubic structure, a systematic study of the electronic structure and the energetics of the fcc-fct structural transition for TiH_2, ZrH_2, and HfH_2 is needed in order to have a better understanding of the nature of the tetragonal distortion in this group of dihydrides. Ultimately, the study of the structural instability of these compounds may contribute to a better understanding of the broader problem: what makes solids unstable?

The aim of this work is to investigate the electronic structure and the energetics of the fcc-fct structural transition for TiH_2, ZrH_2, and HfH_2 by performing highly accurate total-energy calculations as a function of the c/a ratio. Furthermore, in order to evaluate the spin-orbit effects in HfH_2, the calculations for this system were performed in two schemes: first by applying the scalar relativistic approximation (SR) and second by taking into account the spin-orbit coupling (SO). The validity of the Jahn-Teller model in explaining the tetragonal distortion in HfH_2 is evaluated by analyzing the calculated electronic band structure of the cubic phase calculated including the spin-orbit coupling.

II. COMPUTATIONAL DETAILS

The Kohn-Sham total energies were calculated self-consistently using the full-potential linearized augmented plane-wave (FP-LAPW) method[28,29] with local orbital extensions as implemented in the WIEN2K code,[30] where the core states are treated fully relativistically, and the semicore and valence states are computed in the scalar relativistic approximation. For HfH_2, we also performed calculations taking into account the spin-orbit coupling for semicore and valence states in order to analyze its effects on the structural and electronic properties. The exchange-correlation potential was evaluated within the generalized gradient approximation (GGA) using the parameter-free form by Perdew, Burke, and Ernzerhof (PBE96).[31] We used muffin-tin radii of 1.3 a.u. for H, 2.1 a.u. for Ti, and 2.3 a.u. for Zr and Hf. For TiH_2, ZrH_2, and HfH_2 (SR), we chose a plane-wave cutoff $R_{\mathrm{MT}}\times K_{\mathrm{max}}=5.0$ and 6.0 for HfH_2 (SO). Inside the atomic spheres, the potential and charge density were expanded in crystal harmonics up to $l=11$. Electronic self-consistency was asummed when the energy difference between the input and output charge densities was less than 1×10^{-6} Ry.

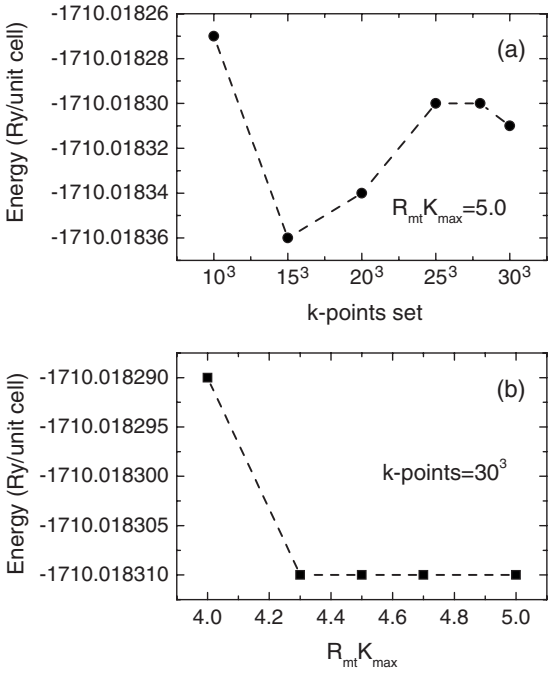

FIG. 1. Total energy per unit formula at the calculated equilibrium lattice constants for TiH_2 in the cubic structure (fcc-CaF_2) as a function of the number of k points (a) and of the $R_{\mathrm{MT}}K_{\mathrm{max}}$ (b).

Special attention was paid to the convergence of the calculations, since previous studies in TiH_2 and ZrH_2 show that the energy differences between the fcc and the fct phases are only a few mRy.[9–11] Figure 1 shows the total energy convergence for TiH_2 in the cubic structure (fcc-CaF_2) as a function of the number of k points and the number of plane waves $R_{\mathrm{MT}}K_{\mathrm{max}}$. We can see that an increase from 25^3 to 30^3 k points in the first Brillouin zone leads to a total-energy difference of 0.01 mRy. Thus, for the three systems the self-consistent procedure were performed with a $30\times30\times30$ k points mesh, which corresponds to 752 k points and 1922 k points in the irreducible part of the first BZ of the fcc and fct structures, respectively. The corrected tetrahedron method[32] with a Gaussian smearing of 0.002 Ry was used for Brillouin- zone integration.

In the first-principles calculations the ions are considered static and quantum mechanical effects are ignored. However, because of the light mass of hydrogen, the magnitude of the zero-point energy becomes comparable to the heat of formation. Indeed, the contribution of zero-point energy vibrations of the hydrogen atoms might be different for the cubic and tetragonally distorted structures of the dihydrides under study. Nevertheless, Miwa and Fukumoto[23] have shown that the zero-point energy correction is important for the quantitative prediction of the heat of formation CaF_2-type transition-metal dihydrides, but this correction has only a small influence on the difference of the heats of formation between the cubic and tetragonal phases. Moreover, Xu and Van der Ven[11] have evaluated the contribution of the vibrational degrees of freedom to the free energy as a function of the c/a for TiH_2 (see Fig. 9 in Ref. 11). For instance, from comparing the total-energy calculations and the free-energy curve for 0 K in Figs. 1 and 9 of the Ref. 11, respectively. It

TABLE I. Lattice parameter (a_0) and bulk modulus (B_0) for TiH_2, ZrH_2, and HfH_2 in the cubic fluorite structure (fcc-CaF_2).

Compound	a_0 (Å)	B_0 (GPa)	Method	Reference
TiH_2	4.428	144	GGA	Present work
	4.454		Expt. (315 K)	3
	4.399	162	LDA	10
	4.414		GGA	11
ZrH_2	4.817	136	GGA	Present work
	4.804	152	LDA	10
HfH_2	4.727	148	GGA (SR)	Present work
	4.690	153	GGA (SO)	Present work

is found that the fct-fcc energy barrier and the magnitude of the tetragonal distortion remain unchanged after the inclusion of the vibrational degrees of freedom at zero Kelvin. Accordingly, the zero-point energy correction were not taken in to account for the present study.

III. RESULTS AND DISCUSSION

For TiH_2, ZrH_2, and HfH_2 in the cubic phase, the total energy was calculated as a function of the cell volume (V) and fitted to the Murnaghan equation of state;[33] from this process the equilibrium volume (V_0) and the bulk modulus (B_0) were obtained. In Table I, we summarize the results for the lattice parameter (a_0) and B_0 of the studied metal dihydrides in the cubic phase (fcc-CaF_2). It is interesting to note that the trend in a_0 and B_0 in this group of compounds is the same as that for Ti, Zr, and Hf in the fcc structure.[34] The calculated lattice parameter for fcc-TiH_2(4.428 Å) is very close to the experimental value (4.454 Å) which was measured at 315 K.[3] Unfortunately, experimental values of the structural properties for ZrH_2 and HfH_2 in the fcc phase are not available in the literature for comparison. Nevertheless, we can see that the present results for TiH_2 and ZrH_2 are in good agreement with previous calculations.[10,11] For HfH_2, we find that the SO coupling induces a small reduction in the lattice parameter (0.8%) and increases the bulk modulus by ~3% (see Table I). Thus, the SO coupling has a small effect on the structural properties of fcc-HfH_2.

The mechanical stability of the cubic phase under tetragonal distortion was evaluated by calculating the total energy as a function of volume conserving tetragonal strain at the calculated equilibrium lattice parameter and preserving the fractional atomic coordinates of the cubic phase.[35,36] This fixing of the fractional coordinates is a consequence of symmetry. The tetragonal phase has spacegroup $I4/mmm$ (No. 139), with the transition-metal atom (Ti, Zr, or Hf) on site $2a$ $(4/mmm)$ and H on site $4d$ $(\bar{4}m2)$. These sites have fixed coordinates (0,0,0) and (0,1/4,1/2) in the tetragonal cell, so there are no free internal structural parameters even with the distortion. We found that when the cubic symmetry of the fcc phase is broken by the tetragonal distortion, the total energy of the three systems decreases, indicating that at low temperatures TiH_2, ZrH_2, and HfH_2 in the cubic phase are intrinsically unstable against tetragonal strain. The results for the total energy as a function of the c/a ratio at constant volume (V_0) for TiH_2, ZrH_2, and HfH_2 are presented in Fig. 2. We can see that for the three dihydrides the total energy shows an asymmetric double minimum structure with a maximum at $c/a=1$. In all cases, the deeper minimum is at $c/a<1$, in agreement with the experimental observations.[2–6,8]

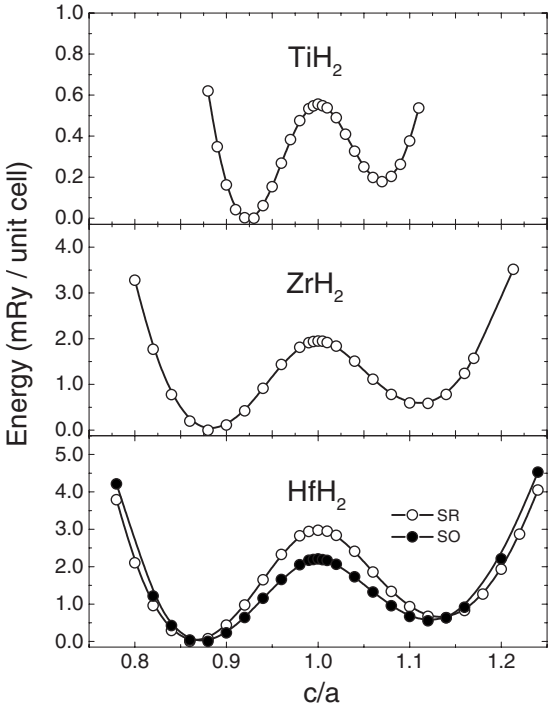

FIG. 2. Total energy as a function of the c/a ratio for TiH_2, ZrH_2, and HfH_2 (SR and SO) in the tetragonally distorted fluorite structure (fct-CaF_2).

In Table II, we show a comparison of the calculated structural parameters for TiH_2, ZrH_2, and HfH_2 in the tetragonal phase (a and c) with previous calculations and experimental data available in the literature. The present calculations predict a c/a ratio for TiH_2 and ZrH_2 that ranges within 1%–2% of the experimental value. For HfH_2, the difference of the calculated c/a including the SO coupling with respect to the experimental value is not larger than 3%. It is interesting to note that for HfH_2, the SO calculations predict lattice parameters smaller than those obtained with the SR approximation. These results show that the SO coupling enhance the bond properties in HfH_2. Thus, we found very good agreement of the calculated tetragonal distortion (c/a) in the present work with the experimental values for the three studied dihydrides.

The fct-fcc energy barrier (ΔE_0) obtained from the scalar relativistic calculations for TiH_2, ZrH_2, and HfH_2 is 0.56, 1.95, and 2.97 mRy, respectively. It is interesting to note that the addition of the SO coupling terms in the case of HfH_2 reduces ΔE_0 from 2.97 to 2.20 mRy, but does not change the trend of ΔE_0 in this group of dihydrides. In view of the tiny fct-fcc energy barrier for TiH_2 (0.56 mRy), the convergence of ΔE_0 with the number of k points was evaluated. Figure 3 shows the convergence of the fct-fcc energy barrier for TiH_2

TABLE II. Lattice parameters (a_0 and c_0) for TiH_2, ZrH_2, and HfH_2 in the tetragonally distorted fluorite structure (fct-CaF_2).

Compound	a_0 (Å)	c_0 (Å)	c/a	Method	Reference
TiH_2	4.554	4.210	0.925	GGA	Present work
	4.528	4.279	0.945	Expt. (79 K)	3
	4.480	4.347	0.970	GGA	23
	4.532	4.187	0.924	GGA	11
ZrH_2	5.021	4.432	0.883	GGA	Present work
	4.985	4.430	0.889	Expt. (79 K)	3
	4.975	4.447	0.894	Expt. (150 K)	8
	4.982	4.449	0.893	Expt. (293 K)	4
	5.008	4.419	0.894	LDA	10
	5.000	4.450	0.890	GGA	9
HfH_2	4.959	4.294	0.866	GGA (SR)	Present work
	4.920	4.291	0.872	GGA (SO)	Present work
	4.882	4.384	0.898	Expt. (300 K)	2

as a function of the number of k points. We can see that an increase from 25^3 to 30^3 k points in the first Brillouin zone leads to a total-energy difference of less than 0.01 mRy, which is one order of magnitude lower that the calculated values for ΔE_0. Now, assuming that the fct-fcc energy barrier in these hydrides is related to the critical temperature (T_c) of the tetragonal-cubic structural transition, it is expected that TiH_2 will be the compound with the lowest T_c of the three hydrides studied, and that the T_c of ZrH_2 and HfH_2 must be roughly similar. The cubic phase of TiH_2 is observed above ~300 K (Ref. 3) and unfortunately there are no reports of T_c for ZrH_2 and HfH_2. Nevertheless, is important to note that the experimental studies of the structural properties of ZrH_2 for temperatures as high as 778 K do not show signals of the tetragonal-cubic structural transformation,[3] indicating that if the fct-fcc transformation occur in ZrH_2 and HfH_2, this will be at higher temperatures. Thus, the trend of the calculated ΔE_0 is in qualitative agreement with the experimental observations of the tetragonal-cubic structural transition for these hydrides. This is also seen in our calculations where we find quantitative agreement for the magnitude of the tetragonal c/a ratios and a substantially smaller energy associated with the distortion of TiH_2 than for ZrH_2 or HfH_2. This is as may be expected from general trends going from $3d$ to $4d$ and $5d$ compounds. In particular, the more extended d orbitals of the $4d$ and $5d$ elements lead to more overlap and stronger electron-phonon coupling.

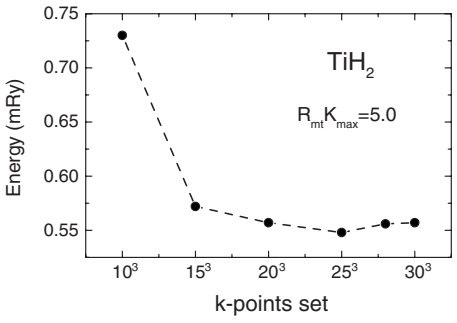

FIG. 3. Energy barrier for TiH_2 in the tetragonally distorted fluorite structure (fct-CaF_2) as a function of the number of k points (see text).

In Fig. 4, we show the band structure for TiH_2, ZrH_2, and HfH_2 in the cubic phase. From an analysis of the band character, we have observed that the states around and above the Fermi level (E_F) are mainly due to the d orbitals of the transition metals. The most relevant band for the discussion of the tetragonal distortion in these dihydrides in the context of the Jahn-Teller model is the doubly-degenerate band in the $\Gamma-L$ direction, which lies just at the Fermi level.[10,19,23,24] We found that in the three compounds, this band is below E_F at Γ and L and above the Fermi level in a small intermediate region between this two high-symmetry points. It is interesting to note that in TiH_2, this band shows hybridization at the Γ point with a lower-energy band, while for ZrH_2 and HfH_2 the hybridization occur with a band of higher energy. In the $\Gamma-K$ path there is a band below E_F that shows a maximum exactly at the Fermi level, which is a so-called van Hove singularity. In order illustrate these two common features of the band structure more clearly, Fig. 5 shows the bands around E_F in the $\Gamma-L$ and $\Gamma-K$ directions for the three dihydrides.

As we mentioned before, several previous reports have suggested that the tetragonal distortion in these hydrides is driven by the Jahn-Teller effect, which is associated to the degeneracy of the band in the $\Gamma-L$ direction at Fermi level.[10,19,23,24] However, as we can see in Fig. 5, the calculation of the band structure for fcc-HfH_2 including the spin-orbit interaction shows that the degeneracy of the band at E_F in the $\Gamma-L$ direction is lifted by this interaction. In this context, the Jahn-Teller model is no longer valid to explain the tetragonal distortion in HfH_2. In contrast, the van Hove singularity in the $\Gamma-K$ direction at Fermi energy in HfH_2 remains unchanged after including the SO interaction.

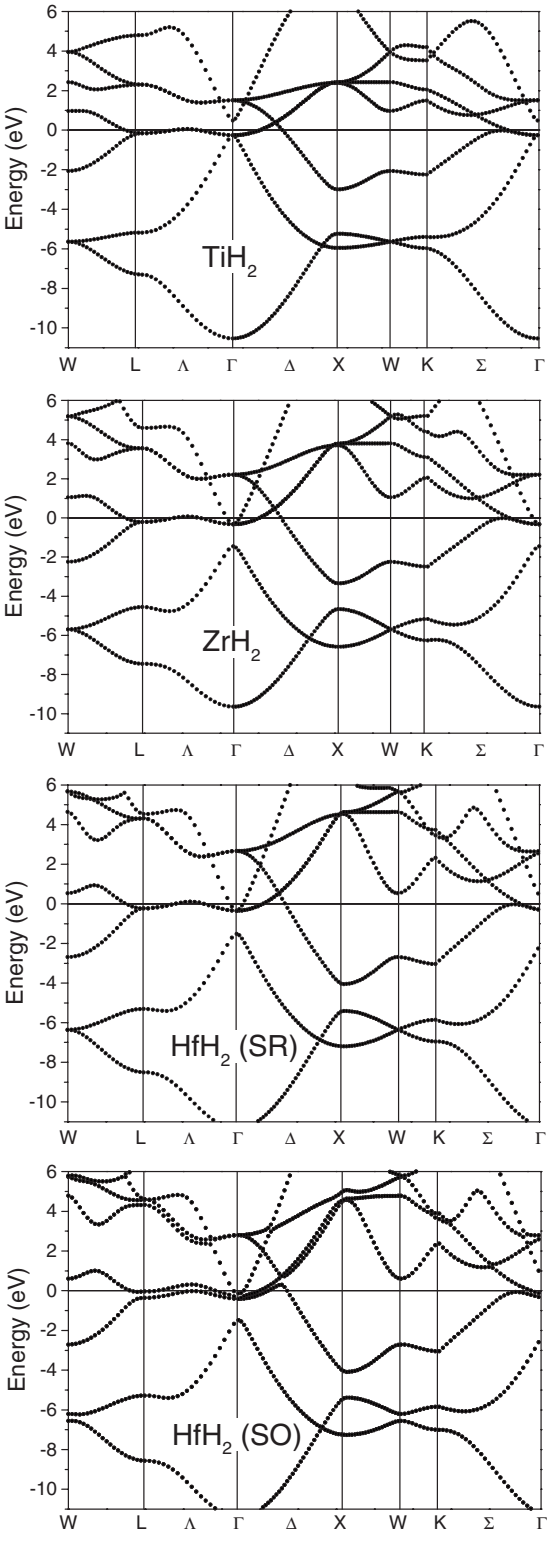

FIG. 4. Electronic band structure for TiH_2, ZrH_2, and HfH_2 (SR and SO) in the cubic fluorite structure (fcc-CaF_2). The zero of the energy axis is at the Fermi level (E_F).

In order to analyze the effect of the tetragonal distortion on the band structure, Fig. 6 shows the calculated band structure for TiH_2, ZrH_2, and HfH_2 in the tetragonal structure ($c/a<1$) for the calculated lattice parameters in Table II. The high-symmetry points W and K in the cubic structure, are no longer high-symmetry point in the tetragonal structure, for this reason that points are primed in the Fig. 6. From the band structure calculations using the SR approximation, we observe that the reduction in the lattice symmetry, caused by the tetragonal distortion of the cubic lattice, splits the doubly degenerate band in the $\Gamma-L$ direction, shifting one of the bands below and one to above E_F. However, the nature of this splitting in TiH_2 is different than that for ZrH_2 and HfH_2. In TiH_2 the band splitting in L and Γ is 0.6 and 0.34 eV, respectively. In contrast, in ZrH_2 and HfH_2 the band splitting in the L point is 1.28 and 1.65 eV, respectively, but there is no band splitting at the Γ point. This result seems to suggest that the details of the electronic mechanism driving the tetragonal distortion in TiH_2 could be different than for ZrH_2 and HfH_2. However, if we focus on the behavior of the van Hove singularity at E_F in the $\Gamma-K$ path, we find that for the three systems including HfH_2 (SO), the tetragonal distortion shifts the van Hove singularity to above of the Fermi level, producing a strong reduction in $N(E_F)$. This common behavior suggests that the van Hove singularity could be playing an important role in the mechanism that induces the tetragonal distortion in TiH_2, ZrH_2, and HfH_2.

In Fig. 7, the electronic density of states (DOS) for TiH_2, ZrH_2, and HfH_2 in the cubic and tetragonal ($c/a<1$) phases are presented. The three systems studied show a pseudogap below the Fermi level, which is located at −3.0, −3.4, and −4.0 eV in TiH_2, ZrH_2, and HfH_2, respectively. The states below the pseudogap correspond mainly to the metal-H and H-H bonding states, while the states around the Fermi level are mainly due to the d orbitals of the transition metal. The DOS of TiH_2 in the fluorite structure, which is representative of these three compounds, shows a broad peak extending from approximately −11 to −4 eV with respect to the Fermi energy. This peak accounts for four electrons per formula unit and is derived from Ti(d)-H(s) bonding bands, with some Ti(s) character. Because Ti is less electronegative than H these bands are polarized toward H. In the fluorite structure each Ti is octahedrally coordinated by H with axes along the cubic [111] directions. In the reference frame of these octahedra the split-off peak consists of H(s)-Ti(e_g) bonding states. These e_g states are directed along the cubic [111] directions. The corresponding antibonding states comprise the DOS starting at approximately 4 eV above E_F. The region between −3 and 4 eV is dominated by Ti(t_{2g}) states in the frame of the octahedron. These states are nonbonding with H and are orthogonal to the [111] directed e_g states. As a result, these bands have almost no dispersion along the $\Gamma-L$ (111) directions. On the other hand, the Ti-Ti distance is short, leading to strong dispersion along other directions and a relatively wide band width. As a consequence, there is a strong van Hove peak in the DOS at a t_{2g} electron count of two, which is the actual electron count in stoichiometric TiH_2. As shown in Fig. 8, the Fermi surface of cubic fluorite TiH_2 reflects this structure, and consists of a small cube-shaped electron section around Γ, a hole jungle gym structure enclosing the cube and also centered at Γ, and small compensating ellipsoidal electron sections.

In the cubic phase the Fermi level is located at a sharp peak of the DOS in the three systems TiH_2, ZrH_2, and HfH_2. It is interesting to note that in HfH_2, the spin-orbit coupling

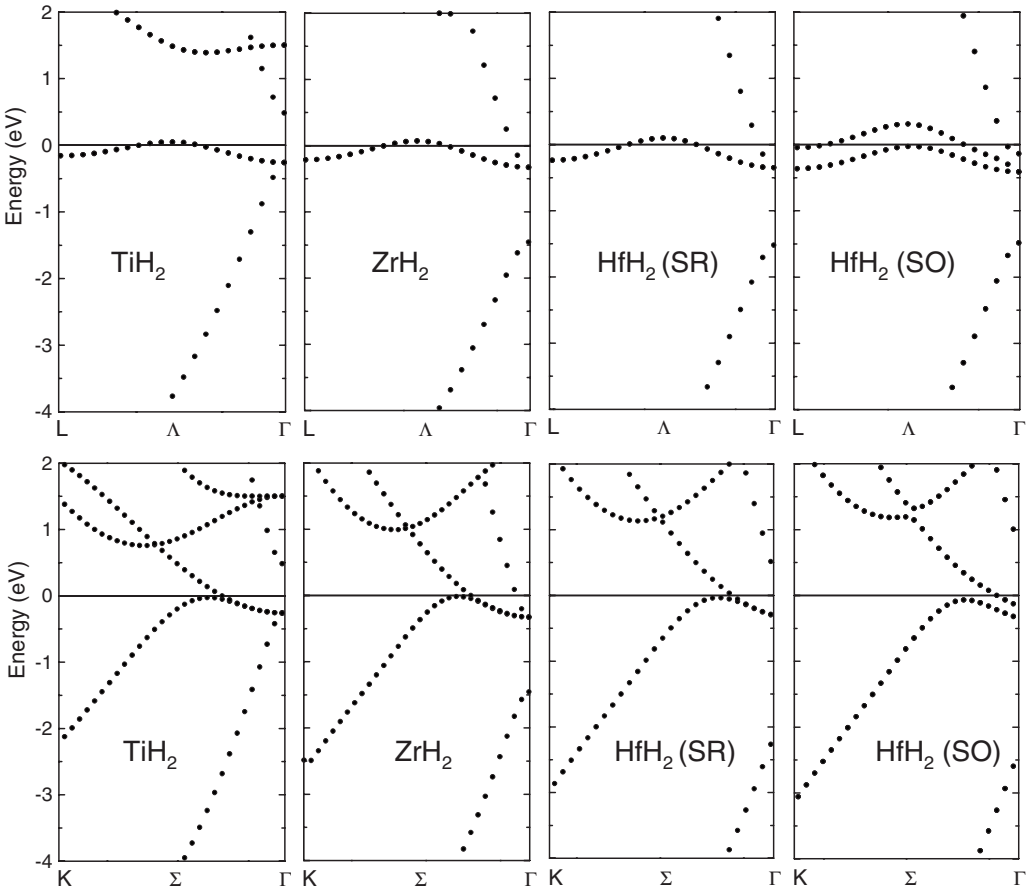

FIG. 5. Electronic band structure for TiH_2, ZrH_2, and HfH_2 (SR and SO) in the cubic fluorite structure (fcc-CaF_2), for the states around the Fermi level in the $\Gamma-L$ (top) and $\Gamma-K$ (bottom) paths, respectively. The zero of the energy axis is at the Fermi level (E_F).

produces a splitting of the peak at E_F in the SR calculation, but a high DOS remains at E_F in HfH_2 (SO). Thus, the spin-orbit coupling in fcc-HfH_2 produces a reduction in the DOS at E_F from 1.6 to 1.1 states/eV unit cell. In contrast, we found that the tetragonal distortion induces a strong reduction in the DOS at the Fermi level in the three cases, resulting from the splitting of the degenerate bands around E_F and the shift of the van Hove singularity in the $\Gamma-K$ path to above E_F. Because the tetragonal distortion in ZrH_2 and HfH_2 is larger than that for TiH_2 (see Table II), the effects of this deformation on the reduction in the DOS at E_F is stronger in ZrH_2(73%) and HfH_2 (71% for RS) than in TiH_2(63%). Hence, the Fermi level in the tetragonal phase is not located at a peak of the DOS but at a local minimum, which leads to a reduction in the electronic contribution to the total energy. As emphasized previously by Ducastelle and by Gupta[12,17] the strong reduction in $N(E_F)$ inferred from electronic specific heat and magnetic susceptibility measurements are indicative of a removal of states from the Fermi surface, and support the model of Gupta,[19] i.e., an instability associated with the peak (van Hove singularity) in the DOS at E_F. In fact, in the absence of distortion, the value of the density of states at the Fermi energy for TiH_2 of 2.6 states/eV unit cell would make it a significant Stoner renormalized paramagnet, while the tetragonal value of 1.0 states/eV unit cell places the low temperature structure far from magnetism, which would then yield simple Pauli paramagnetic behavior. Similarly, there are strong reductions in $N(E_F)$ for ZrH_2 and HfH_2 upon formation of the tetragonal structure, to ~0.5 and 0.4 states/eV unit cell, respectively. Thus, the present results suggest that the structural instability of TiH_2, ZrH_2, and HfH_2 in the fcc structure is due to a van Hove singularity. It is important to mention that structural instabilities induced by van Hove singularities have also been observed in other compounds such as EuPdP,[37] the Ni_xAl_{1-x} alloys,[38,39] and cuprates.[40–42]

Finally, we want to emphasize that in contrast to TiH_2 and ZrH_2, the band structure for fcc-HfH_2 including the spin-orbit interaction does not show a doubly degenerate band at E_F in the $\Gamma-L$ direction. Hence, the Jahn-Teller model is not suitable to explain the observed tetragonal distortion in HfH_2. Thus, the present calculations call for a revision of the mechanism inducing the tetragonal distortion in the TiH_2, ZrH_2, and HfH_2 hydrides.

IV. CONCLUSIONS

We have performed highly accurate first-principles calculations of the electronic structure and energetics of the tetragonal distortion for the fluorite-type dihydrides TiH_2, ZrH_2, and HfH_2. For HfH_2 the spin-orbit coupling effects on the electronic structure and energetics have been analyzed. The total-energy calculations show that the three systems are

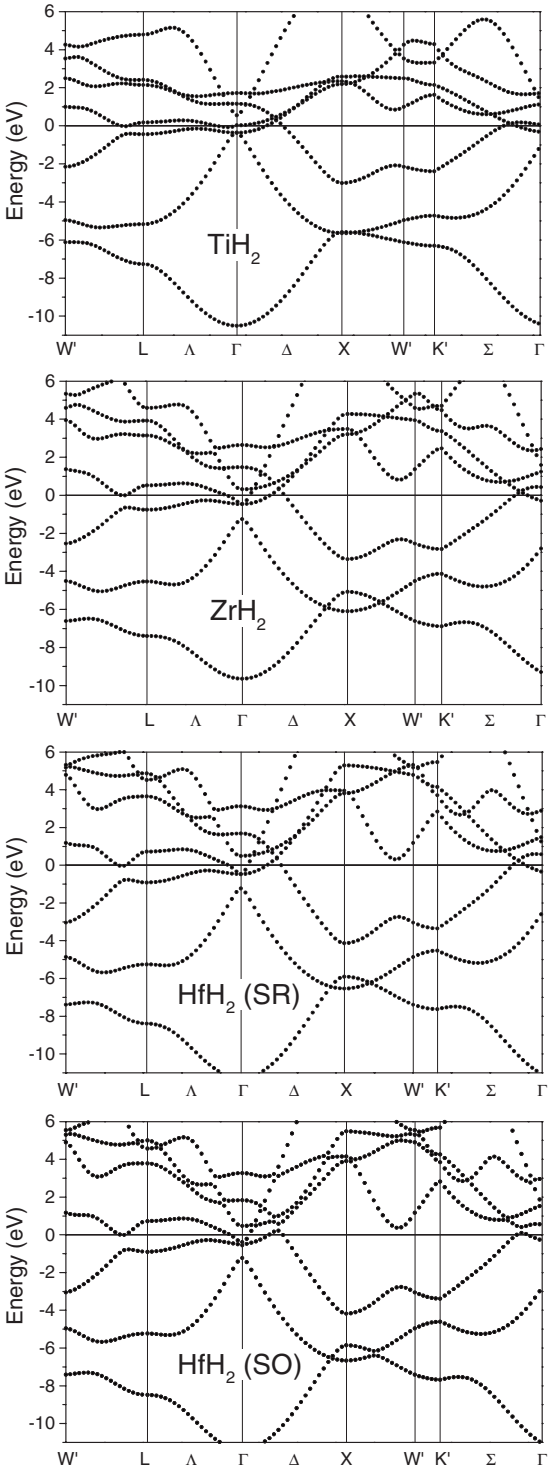

FIG. 6. Electronic band structure for TiH_2, ZrH_2, and HfH_2 (SR and SO) in the tetragonally distorted fluorite structure (fct-CaF_2) with $c/a<1$ (see Table II). The zero of the energy axis is at the Fermi level (E_F).

unstable in the cubic phase and that the ground state of these dihydrides corresponds to a tetragonal distorted fluorite structure with $c/a<1$, in agreement with experimental observations. The band structure of TiH_2, ZrH_2, and HfH_2 (SR) show a nearly flat doubly degenerate band in the $\Gamma-L$ direction which crosses the Fermi level twice, and a van Hove

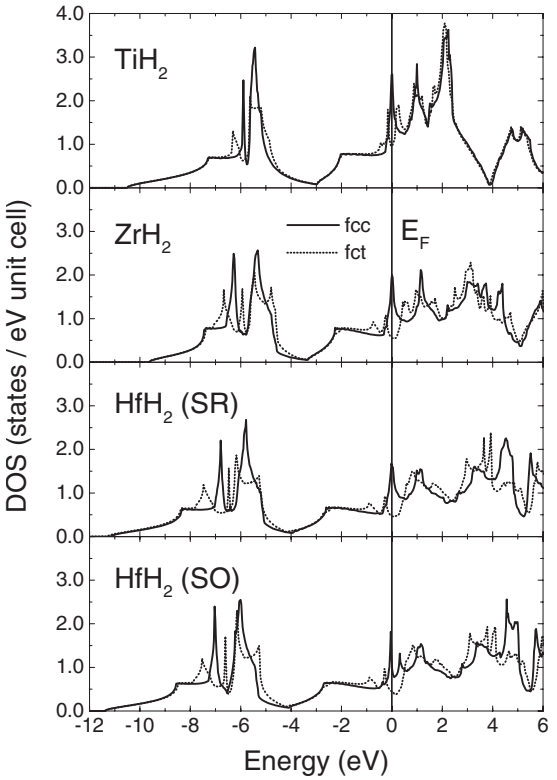

FIG. 7. Electronic density of states for TiH_2, ZrH_2, and HfH_2 (SR and SO) in the cubic fluorite structure (fcc-CaF_2, solid line) and the tetragonally distorted fluorite structure (fct-CaF_2, dashed line) with $c/a<1$ (see Table II). The zero of the energy axis is at the Fermi level (E_F).

singularity exactly at E_F in the $\Gamma-K$ path. We find that the tetragonal distortion splits the doubly degenerate band at E_F in the $\Gamma-L$ direction and shift the van Hove singularity to above the Fermi level. Thus the tetragonal distortion splits the peaks at E_F in the DOS and lowers the energy. In TiH_2 and ZrH_2 this behavior has been referred to as a Jahn-Teller mechanism in analogy with the molecular case where a symmetry lowering distortion may be driven by degeneracy of a partly occupied state. However, it should be emphasized that the van Hove peak of the undistorted systems arises from states in a small region in reciprocal space, and hence it is perhaps useful to describe the distortion as being driven by a Fermi surface instability.

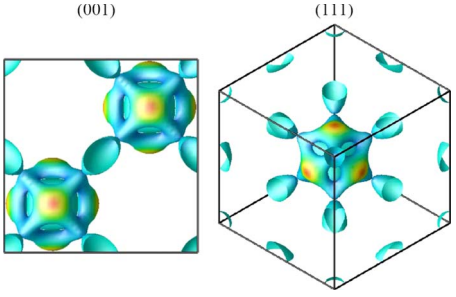

FIG. 8. (Color online) Fermi Surface of TiH_2(fcc) shown in an extended zone scheme. Relative to the cube depicted, the Γ points are at (1/4, 1/4, 1/4) and (3/4, 3/4, 3/4).

Regarding to the spin-orbit effects in fcc-HfH_2, we found that the spin-orbit coupling lifts the degeneracy of the partially filled bands in the $\Gamma - L$ direction at the Fermi level with respect to the scalar relativistic calculation. Hence, the Jahn-Teller model is not suitable to explain the tetragonal distortion in HfH_2, since the requirement of a degenerate band at the Fermi level is not satisfied in this particular case. However, the van Hove singularity in the $\Gamma - K$ path remains very close to the Fermi level. Therefore, in fcc-HfH_2 (SO) there is still a prominent peak around E_F in the DOS, and this drives the instability in the same way as in TiH_2 and ZrH_2.

ACKNOWLEDGMENTS

The authors would like to thank Gerko Oskam, Edgar Martínez-Guerra, and Omar de la Peña for a critical reading of the manuscript. One of the authors (RQ) gratefully acknowledges Consejo Nacional de Ciencia y Tecnología (CONACYT, México) and CINVESTAV. This research was partially supported by CONACYT-México under Grant No. 25794-J. Work at ORNL was supported by the Department of Energy, Division of Materials Sciences and Engineering.

[1] Y. Fukai, *Metal Hydrogen System. Basics Bulk Properties* (Springer, Berlin, 2005).
[2] S. S. Sidhu and J. C. MacGuire, J. Appl. Phys. **23**, 1257 (1952).
[3] H. L. Yakel, Acta Crystallogr. **11**, 46 (1958).
[4] R. C. Bowman, E. L. Venturini, B. D. Craft, A. Attalla, and D. B. Sullenger, Phys. Rev. B **27**, 1474 (1983).
[5] R. C. Bowman,Jr. and B. D. Craft, J. Phys. C **17**, L477 (1984).
[6] R. C. Bowman, B. D. Craft, J. S. Cantrell, and E. L. Venturini, Phys. Rev. B **31**, 5604 (1985).
[7] O. J. Zogal, B. Nowak, and K. Niedzwiedz, Solid State Commun. **80**, 601 (1991).
[8] K. Niedzwiedz, B. Nowak, and O. J. Zogal, J. Alloys Compd. **194**, 47 (1993).
[9] G. J. Ackland, Phys. Rev. Lett. **80**, 2233 (1998).
[10] W. Wolf and P. Herzig, J. Phys.: Condens. Matter **12**, 4535 (2000).
[11] Q. Xu and A. Van der Ven, Phys. Rev. B **76**, 064207 (2007).
[12] F. Ducastelle, R. Candron, and P. Costa, J. Phys. **31**, 57 (1970).
[13] K. Bohmhammel, G. Wolf, G. Gross, and H. Madge, J. Low Temp. Phys. **43**, 521 (1981).
[14] J. H. Weaver, D. J. Peterman, D. T. Peterson, and A. Franciosi, Phys. Rev. B **23**, 1692 (1981).
[15] A. C. Switendick, J. Less Common Met. **49**, 283 (1976).
[16] M. Gupta, Solid State Commun. **29**, 47 (1979).
[17] M. Gupta, Phys. Rev. B **25**, 1027 (1982).
[18] A. C. Switendick, J. Less Common Met. **101**, 191 (1984).
[19] M. Gupta, Phys. Rev. Lett. **81**, 3300 (1998).
[20] D. A. Papaconstantopoulos and A. C. Switendick, J. Less Common Met. **103**, 317 (1984).
[21] R. S. Gupta and S. Chatterjee, J. Phys. F: Met. Phys. **14**, 631 (1984).
[22] S. E. Kul'kova, O. N. Muryzhnikova, and I. I. Naumov, Phys. Solid State **41**, 1763 (1999).
[23] K. Miwa and A. Fukumoto, Phys. Rev. B **65**, 155114 (2002).
[24] G. Paolucci, E. Colavita, and J. H. Weaver, Phys. Rev. B **32**, 2610 (1985).
[25] O. Jepsen, O. K. Andersen, and A. R. Mackintosh, Phys. Rev. B **12**, 3084 (1975).
[26] B. R. Sahu and L. Kleinman, Phys. Rev. B **72**, 113106 (2005).
[27] N. I. Kulikov, V. N. Bozunov, and A. D. Zvonkov, Phys. Status Solidi **86**, 83 (1978) b.
[28] O. K. Andersen, Phys. Rev. B **12**, 3060 (1975).
[29] D. J. Singh, *Plane Waves, Pseudopotentials, and the LAPW Method* (Kluwer Academic, New York, 1994).
[30] P. Blaha, K. Schwarz, G. Madsen, D. Kvasnicka, and J. Luitz, WIEN2K, *An Augmented Plane Wave + Local Orbitals Program for Calculating Crystal Properties* (Karlheinz Schwarz, Techn. Universität Wien, Austria, 2001).
[31] J. P. Perdew, K. Burke, and M. Ernzerhof, Phys. Rev. Lett. **77**, 3865 (1996).
[32] P. E. Blöchl, O. Jepsen, and O. K. Andersen, Phys. Rev. B **49**, 16223 (1994).
[33] F. D. Murnaghan, Proc. Natl. Acad. Sci. U.S.A. **30**, 244 (1944).
[34] A. Aguayo, G. Murrieta, and R. de Coss, Phys. Rev. B **65**, 092106 (2002).
[35] A. Y. Liu and D. J. Singh, Phys. Rev. B **47**, 8515 (1993).
[36] G. Murrieta, A. Tapia, and R. de Coss, Carbon **42**, 771 (2004).
[37] C. Felser, S. Cramm, D. Johrendt, A. Mewis, O. Jepsen, G. Hohlneicher, W. Eberhardt, and O. K. Andersen, Europhys. Lett. **40**, 85 (1997).
[38] I. I. Naumov and O. I. Velikokhatniy, J. Phys.: Condens. Matter **9**, 10339 (1997).
[39] X. Huang, I. I. Naumov, and K. M. Rabe, Phys. Rev. B **70**, 064301 (2004).
[40] J. D. Jorgensen, H.-B. Schüttler, D. G. Hinks, D. W. Capone II, K. Zhang, M. B. Brodsky, and D. J. Scalapino, Phys. Rev. Lett. **58**, 1024 (1987).
[41] R. S. Markiewicz, J. Supercond. **8**, 579 (1995).
[42] G. Kastrinakis, Physica C **382**, 443 (2002).